Indirect experimental method for constraining the ^{192,193}Ir(n,γ) cross sections

S. P. E. Magagula

1. SSC Laboratory, iThemba LABS P.O. Box 722, Somerset West 7129, South Africa
2. School of Physics, University of the Witwatersrand, Johannesburg 2050, South Africa

This work is based on the research supported by the National Research Foundation of South Africa (Grant Number: PMDS22070734847) and SAINTS Prestigious Doctoral Scholarship.

Introduction and Physics motivation

- Neutron Capture Cross sections – estimated using the Hauser-Feshbach model implemented in the TALYS code
- NLD – Nuclear level density
- GSF – Gamma strength function is a characteristic of the average electromagnetic transition properties of excited nuclei

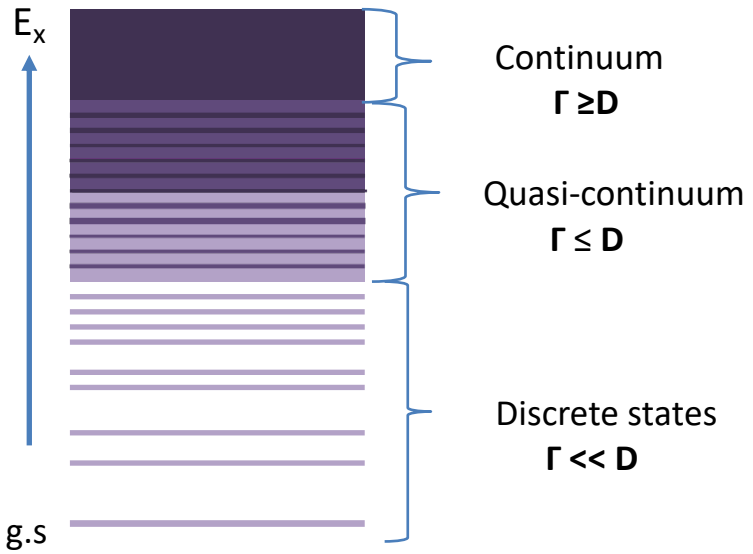

Figure 1: Level density as excitation energy increases

- An approach to constraining cross sections
- Allows us to investigate the s-process branching point ^{192}Ir

Indirect method and why

- Purple - stable
- Light Purple – unstable

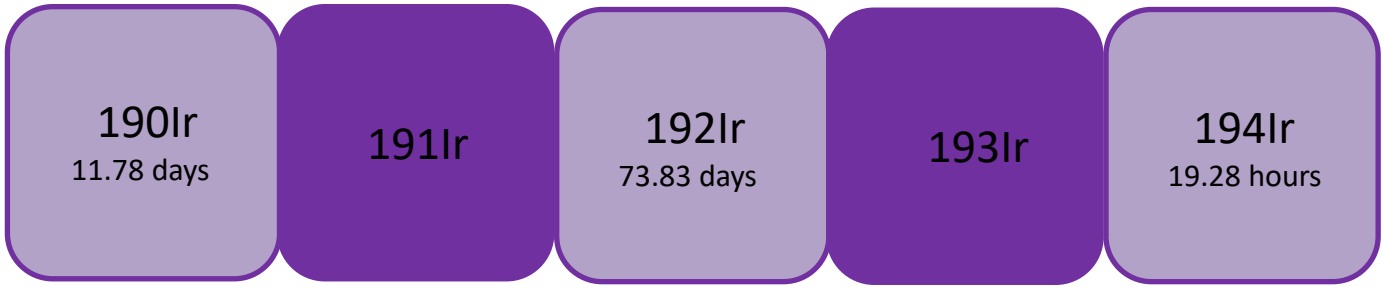

Figure 2: Part of the Iridium isotopic chain and half lives

- ^{192} Ir is unstable, $^{192}Ir(n,\gamma)^{193}Ir$
- $^{192}Os(\alpha,t\gamma)^{193}Ir$
- Use $^{192}Os(\alpha,d\gamma)^{194}Ir$
- $^{193}Ir(n,\gamma)^{194}Ir$

- Heavy element nucleosynthesis calculations and determining the abundances of elements.
- The s- and r-processes are equally responsible for the formation of almost all nuclei heavier than iron
- For the s-process branch-point nuclei, neutron capture cross-section data may not be available or limited to a narrow energy range

The Branching point

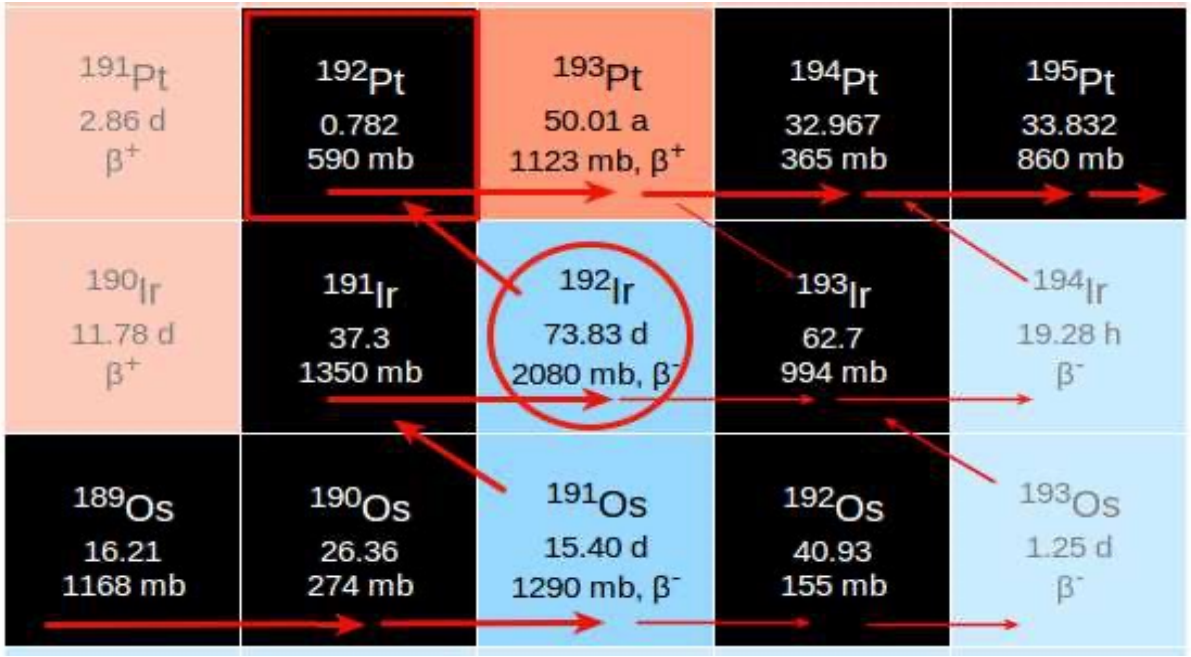

Bisterzo, S, et al. (2015). *Monthly Notices of the Royal Astronomical Society*, *449*(1)

Figure 3: The ^{192}Ir branch feeding the s-only Pt

- Element abundances, e.g Pt, partially depend on ^{192}Ir.
- Provides information on the s-process neutron density (beta decay – neutron capture)

Objectives

- Measure particle-γ coincidences using the ^{192}Os(a,d γ),(a,t γ)
- Extract and normalize the NLD and GSF using the Oslo method
- Use the NLD and GSF to calculate the neutron capture cross section of ^{193,194}Ir
- Compare the ^{194}Ir cross sections with known data to benchmark our approach
- Calculate MACS for ^{193}Ir(n,$\boldsymbol{\gamma}$)^{194}Ir , ^{192}Ir(n,$\boldsymbol{\gamma}$)^{193}Ir
- Use the MACS to evaluate the abundance distribution of the Pt isotopes

➢ NB: ^{193}Ir(n,$\boldsymbol{\gamma}$)^{194}Ir , ^{192}Ir(n,$\boldsymbol{\gamma}$)^{193}Ir

Experimental set up

CACTUS

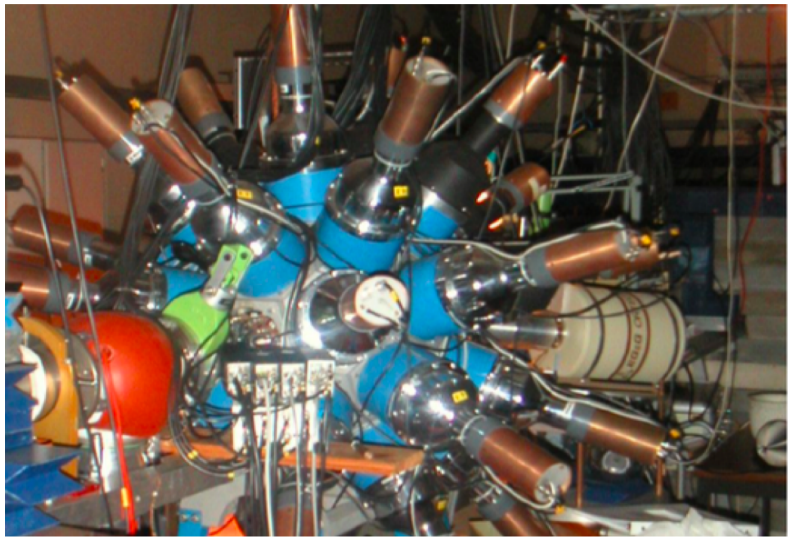

SiRi

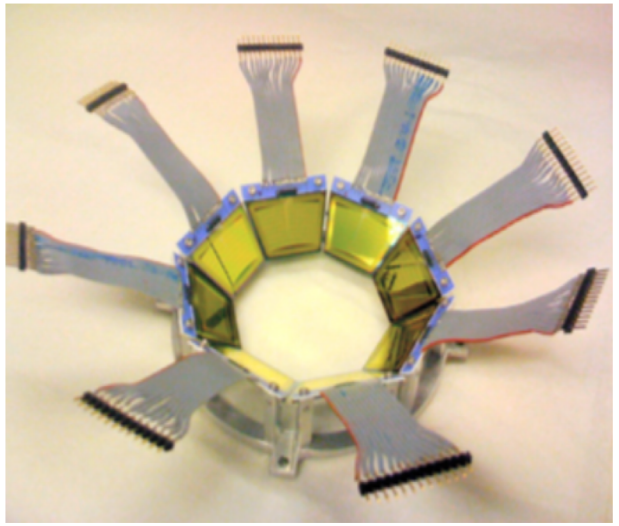

M. Guttormsen, et al. Nucl. Instr and Meth. in Phys doi: 10.1016 (2011)

Figure 4: The gamma ray and particle detectors at the Oslo cyclotron lab and the particle- gamma coincidence.

- Gamma ray detection
- 26 NaI(Tl)
- ^{192}Os(α,d), ^{192}Os(α,t)
- The experiment ran for 5 days
- Charged particle detection
- 64 silicon telescopes placed at backward angels
- 30 MeV beam energy
- With a 0.33mg/cm^2 thick ^{192}Os

Oslo Method

- This is a combination of techniques that enables users to simultaneously extract the NLD and GSF.
- The method takes the coincidence matrix as its starting point, then a set of procedures are subsequently performed, eventually leading to the desired quantities. It consists of the following steps

- Unfolding the coincidence spectrum
  (M. Guttormsen et al. 1996)
- Extract primary gamma-rays
  (M. Guttormsen et al. 1987.)
- Extracting the NLD and GSF
  (A. Schiller et al 2000)
- Normalization

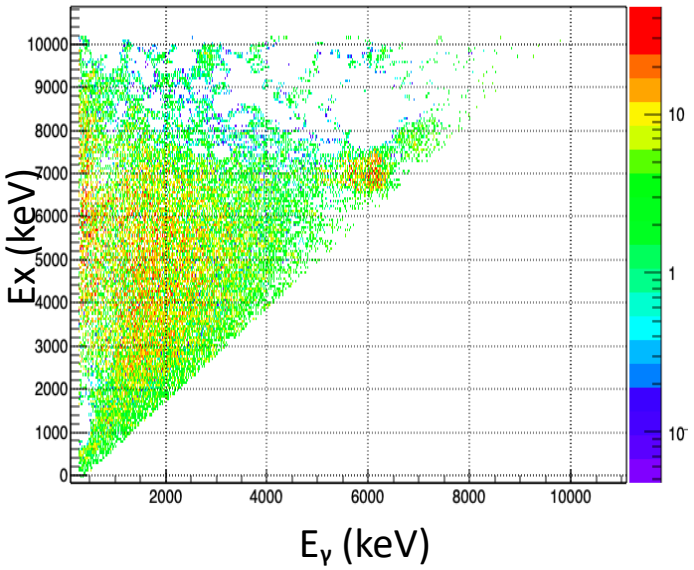

Figure 4.1 The particle-γ matrix of ^{194}Ir

Results

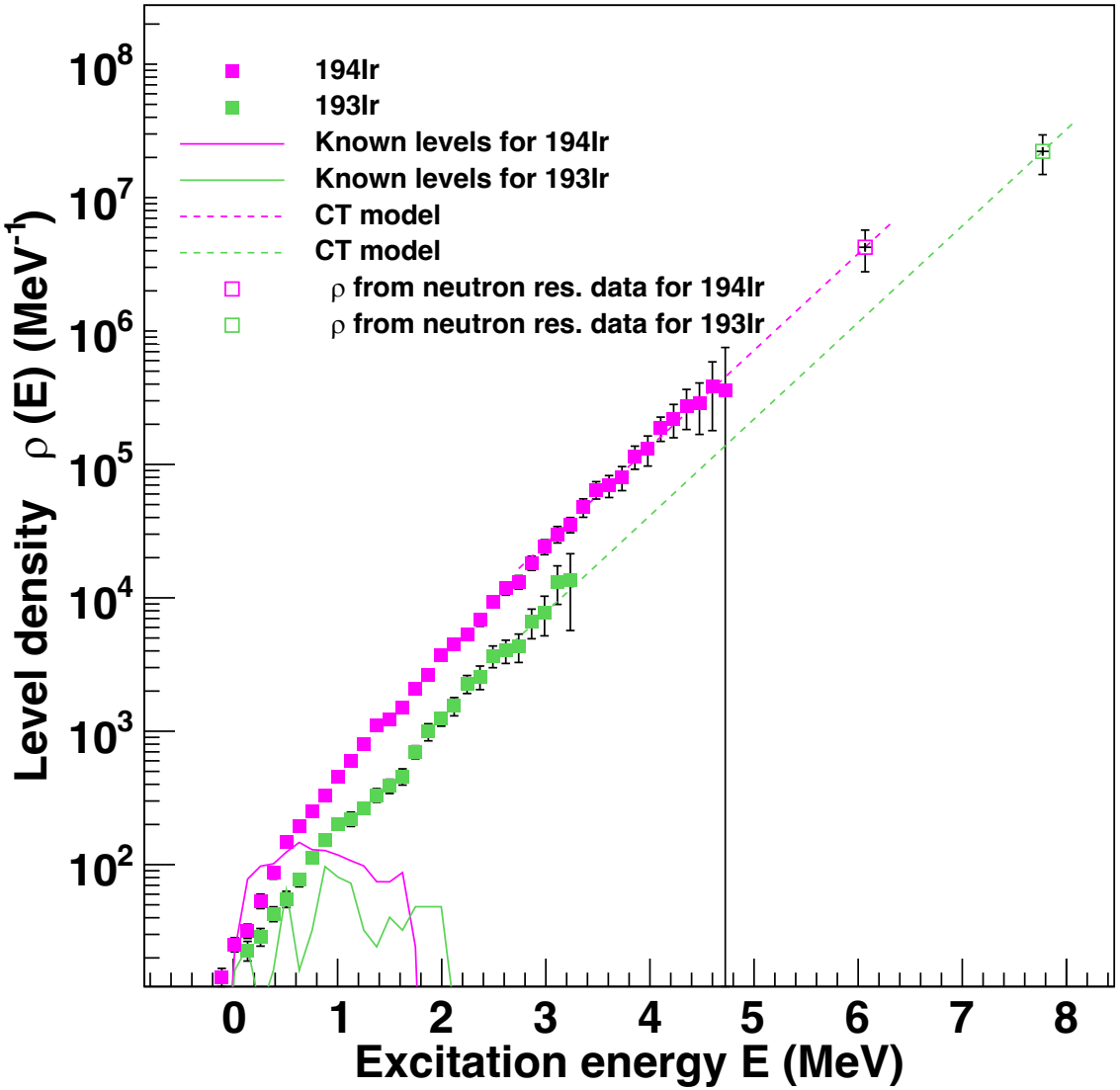

$$\rho(Sn)= \frac{2\sigma^2}{D0} \frac{1}{(I+1)\exp[-\frac{(I+1)2}{2\sigma^2}]+\exp[-\frac{I^2}{2\sigma^2}]}$$

RIPL -2 (Index)- IAEA
Nuclear Data Services
https://www-nds.iaea.org

NNDC
https://www.nndc.bnl.gov/

Figure 5: NLD of ^{193,194} Ir

Results

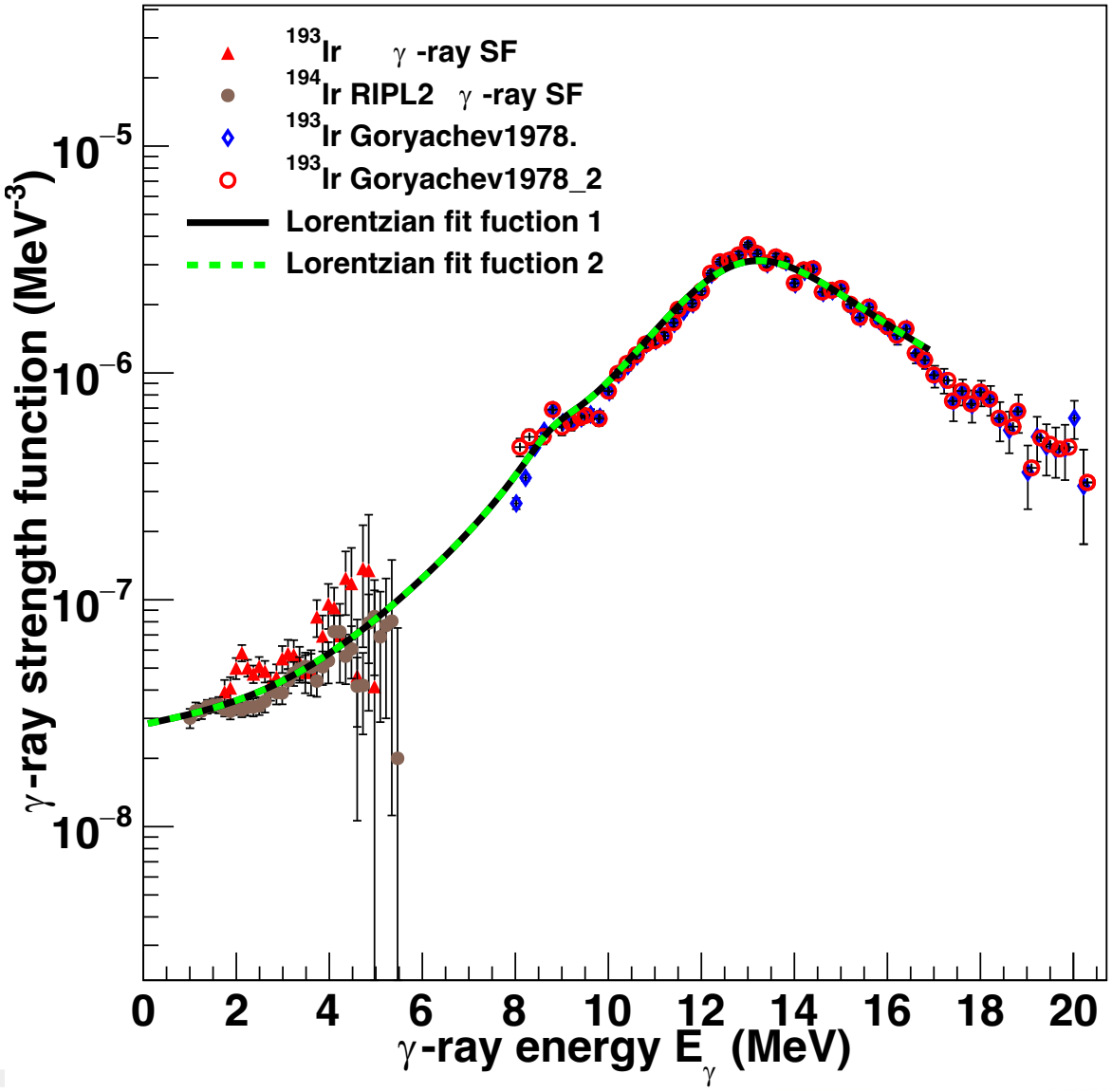

$$fE_\gamma = \frac{1}{2\pi {E_\gamma}^3} BT(E_\gamma)$$

EXFOR: Experimental Nuclear Reaction Data
https://www-nds.iaea.org

Figure 6: GSF of ^{193,194} Ir, Compared to the GDR data

Results- Benchmark calculation

$$\sigma^{\mu}_{n,\gamma}(E^{\mu}_{n}) \approx \frac{\pi\lambda_n^2}{(2J^{\mu}_{i}+1)(2J_n+1)} \sum_{J^{\pi}} (2J+1) \frac{T^{\mu}_{n}(E,J^{\pi}) T^{\mu}_{\gamma}(E,J^{\pi})}{T^{\mu}_{\mathrm{tot}}(E,J^{\pi})}$$

$$T^{\mu}_{\gamma}(E,J^{\pi}) = \sum_{\mu=0,XL} T^{\mu}_{\gamma,XL}(E,J^{\pi}) + \int \sum_{XL} T_{\gamma,XL}(E_{\gamma}) \rho(E-E_{\gamma},J^{\pi}) \cdot dE_{\gamma}$$

GSF

NLD

Hauser Feshbach model

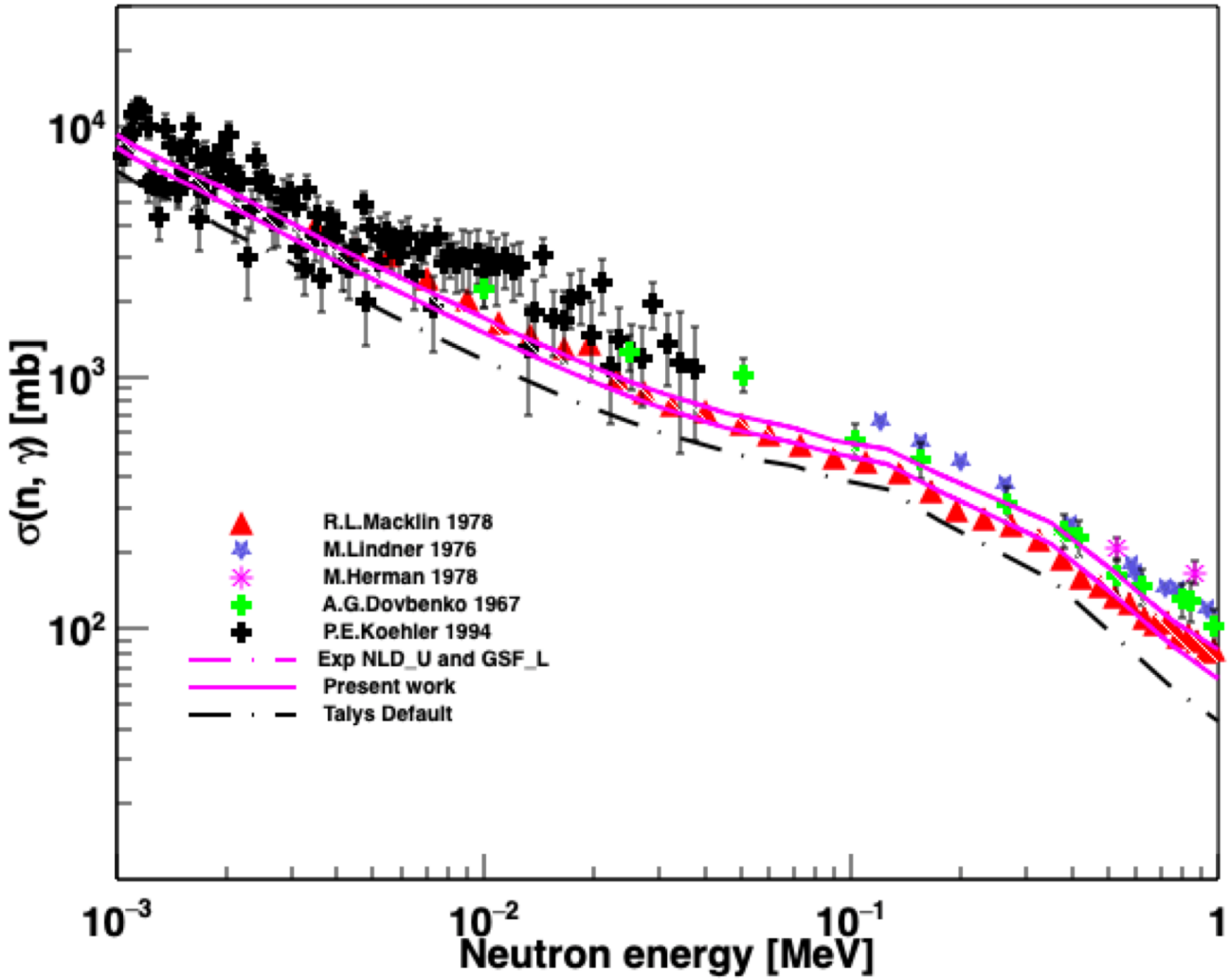

Figure 7: (n,g) cross sections of ^{194} Ir

Benchmark results with available data to compare with, most From EXFOR

Results

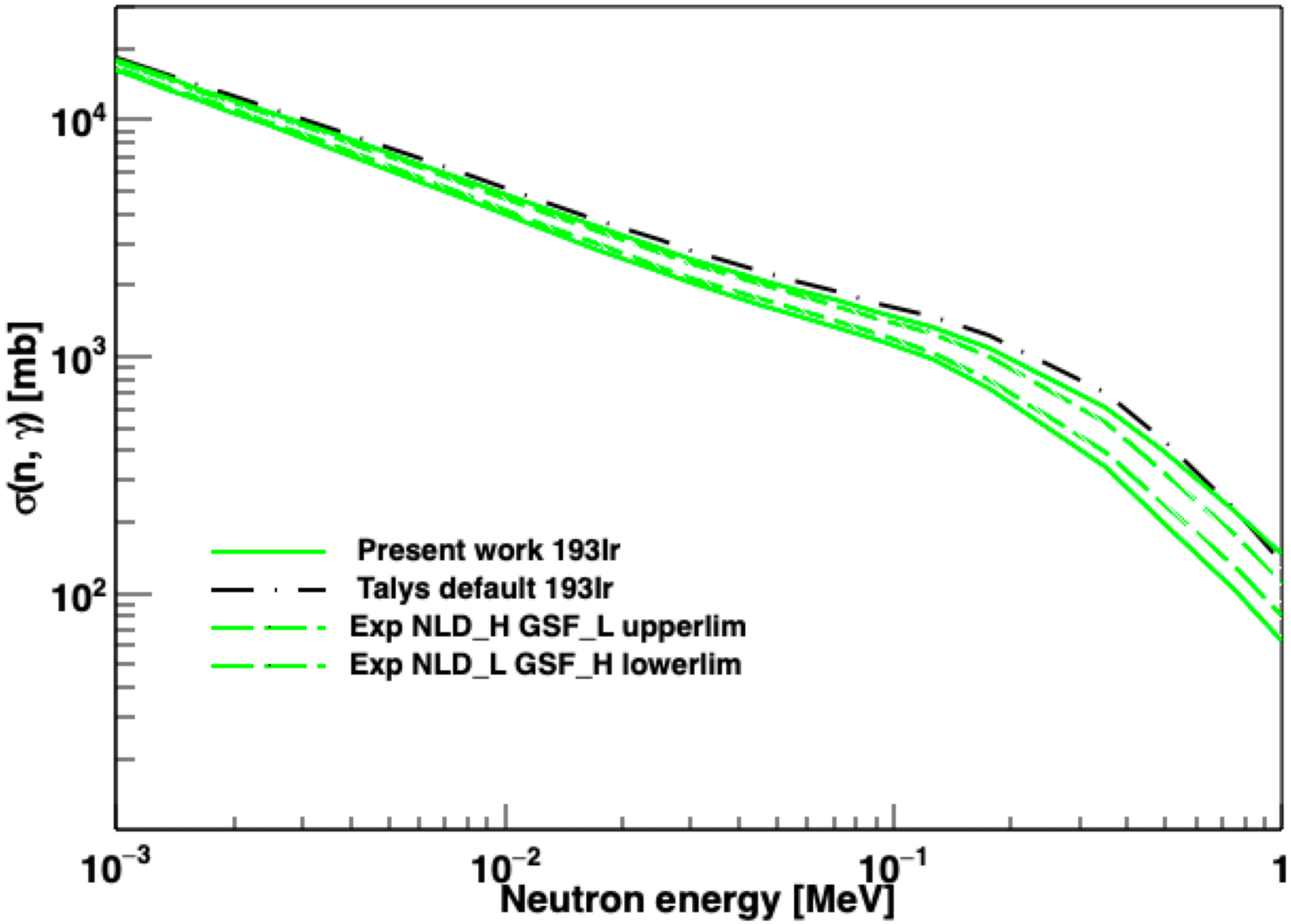

Figure 8: (n,g) cross sections of ^{193}Ir

Results

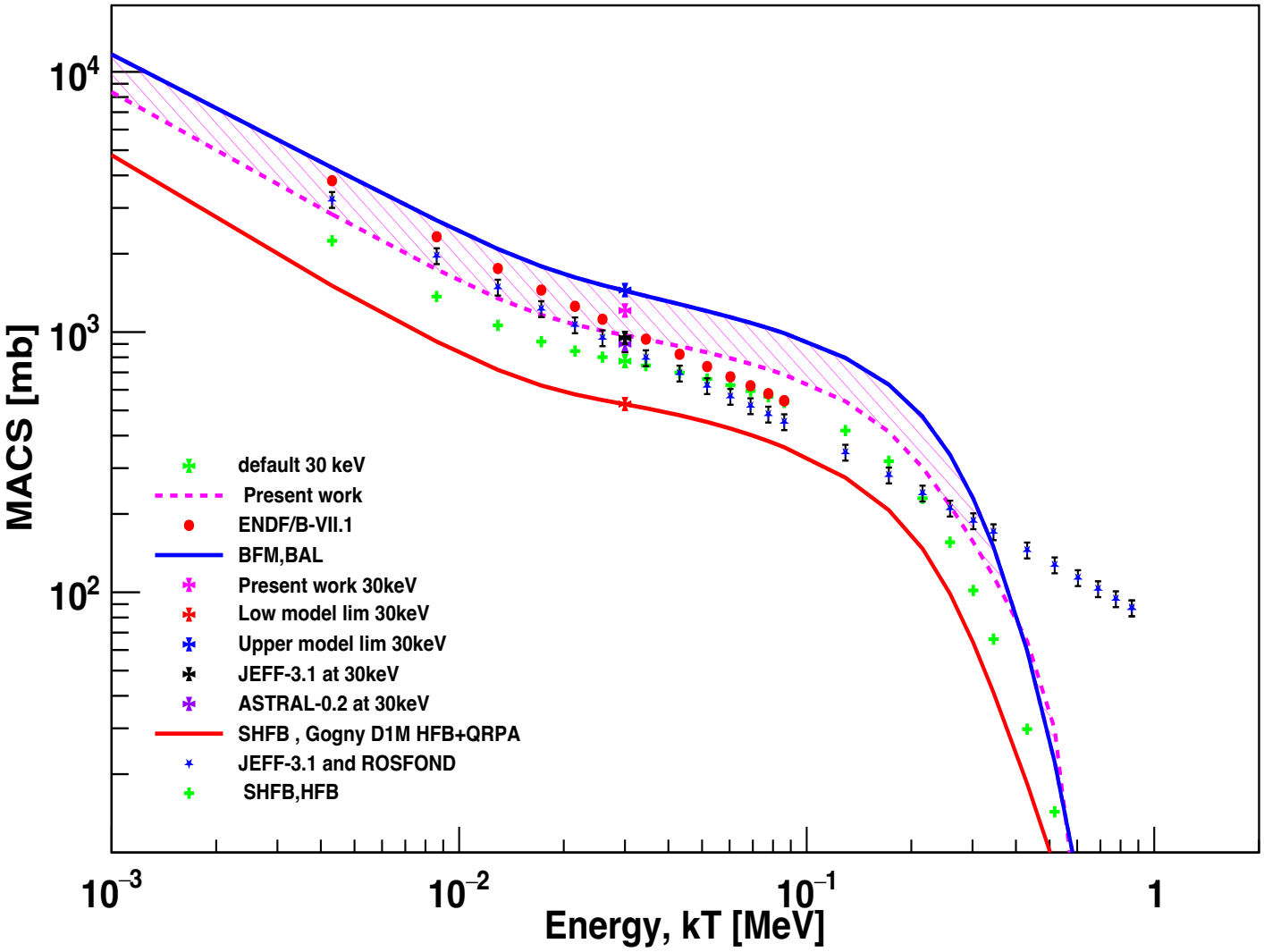

$E_n = kT$

Figure 9: MACS for $^{193}Ir(n,g)^{194}Ir$

Results

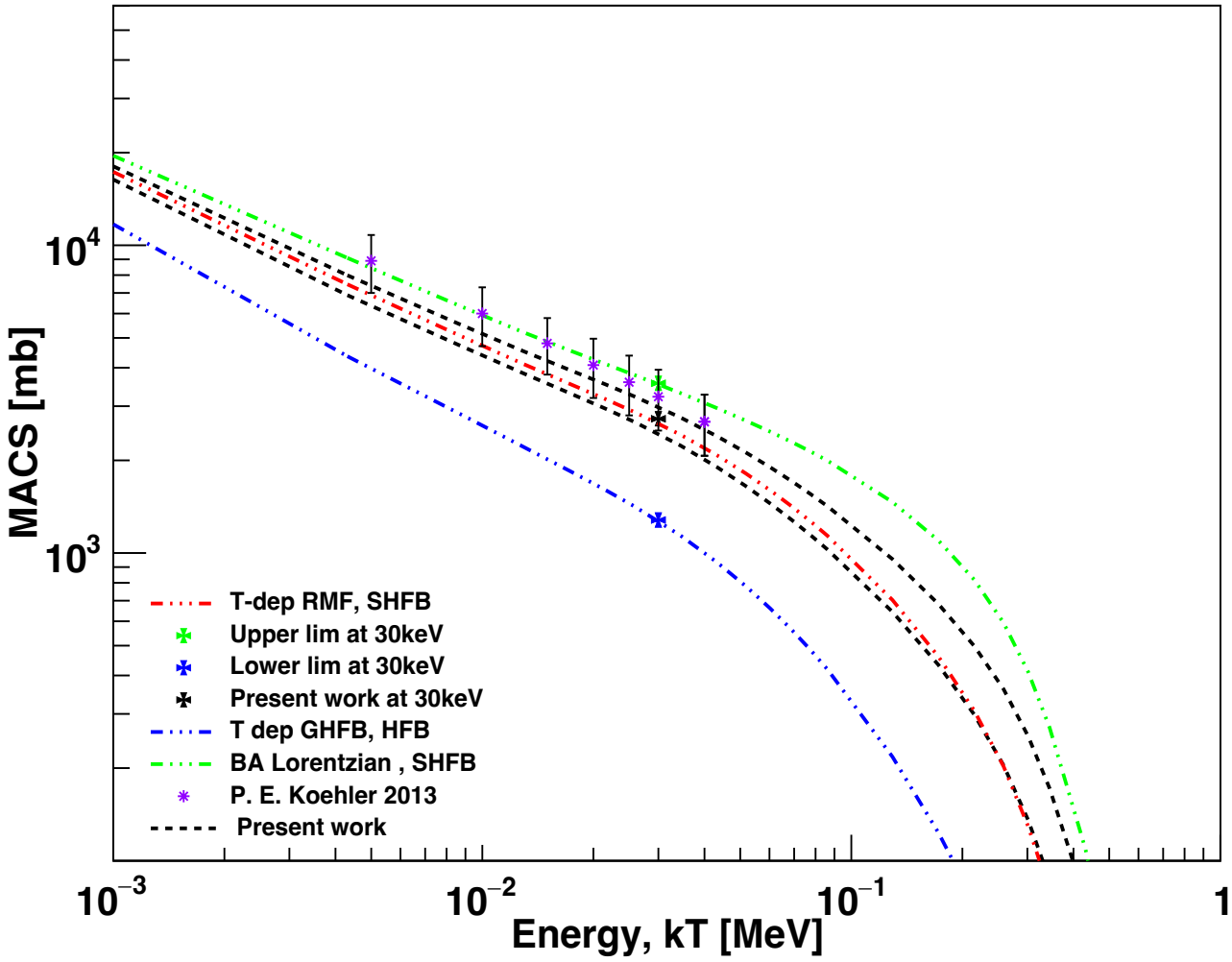

Figure 10: MACS For ^{192}Ir(n,g)

Results

Calculations by S Goreily

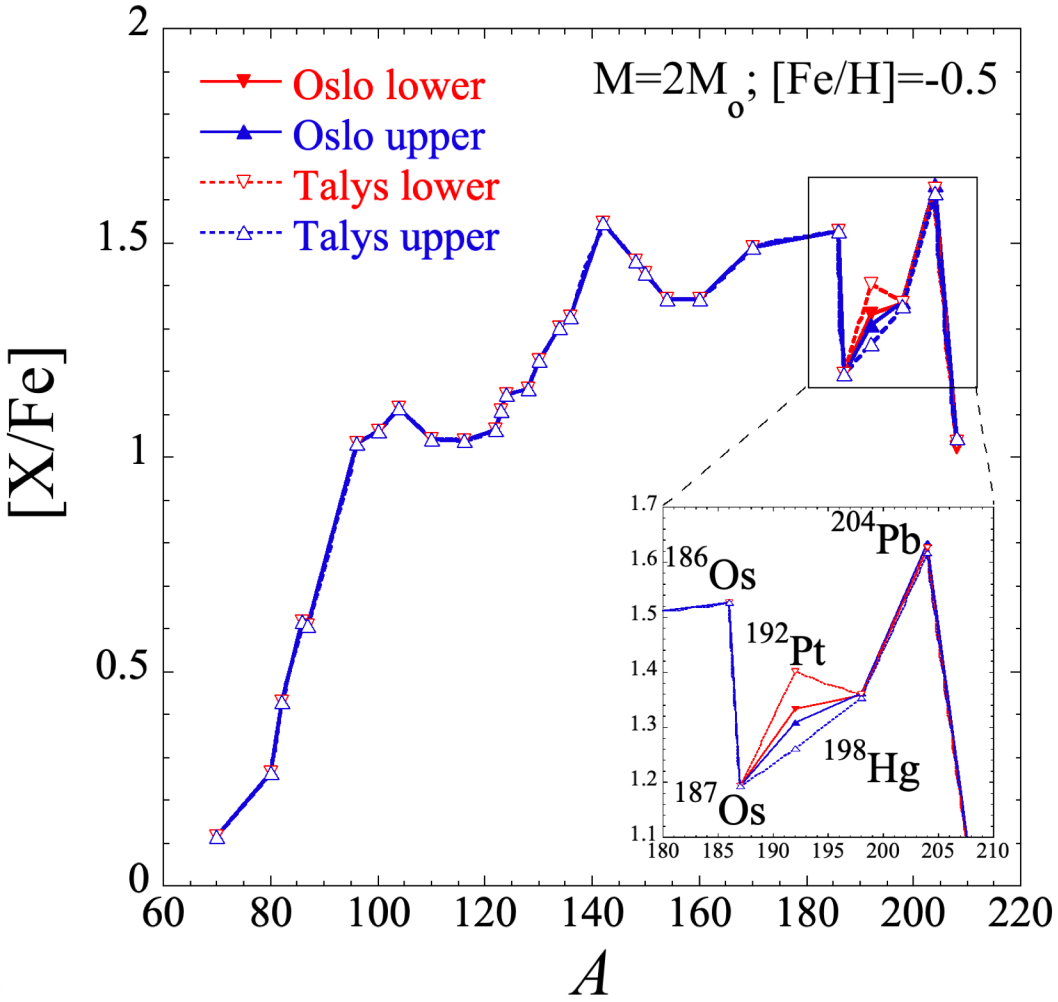

Figure 11: Surface overabundances as a function of the atomic mass A for s-only nuclei at the end of the AGB phase.

Present experimental constraints on the ^{193}Ir NLD and PSF

reduce the uncertainty affecting the production of the s-only ^{192}Pt nucleus by 20 %.

An increase of the ^{192}Ir(n,γ)^{193}Ir , decreases the β-branching of ^{192}Ir and consequently decreases the production of ^{192}Pt.

Summary and Conclusion

- Conducted the ^{192}Os(a,t) and (a,d) experiment to measure particle-γ coincidence for ^{193,194}Ir
- Experimental NLD and GSF were extracted for ^{193,194}Ir
- Experimentally constrained ^{192}Ir(n,γ)Ir^{193} MACS and reduced the error band by 20%.
- S Goriely performed s-process calculations to determine the abundance distribution of the s-only isotopes affected by the ^{192}Ir branching point. A decrease in the ^{192}Ir(n, γ) increases the production of ^{192}Pt.

Acknowledgments

M. Wiedeking

BERKELEY LAB
LAWRENCE BERKELEY NATIONAL LABORATORY

NRF National Research Foundation | iThemba LABS Laboratory for Accelerator Based Sciences

B. V Kheswa

UNIVERSITY OF JOHANNESBURG

K. L Malatji

L Pellegri

THE UNIVERSITY OF CALIFORNIA BERKELEY 1868

ULB UNIVERSITÉ LIBRE DE BRUXELLES

UNIVERSITY OF THE WITWATERSRAND JOHANNESBURG

S . Goriely

UNIVERSITAS OSLOENSIS MDCCCXI

UNIVERSITY OF OSLO

A.C Larsen

science & innovation
Department:
Science and Innovation
REPUBLIC OF SOUTH AFRICA

Back up slides

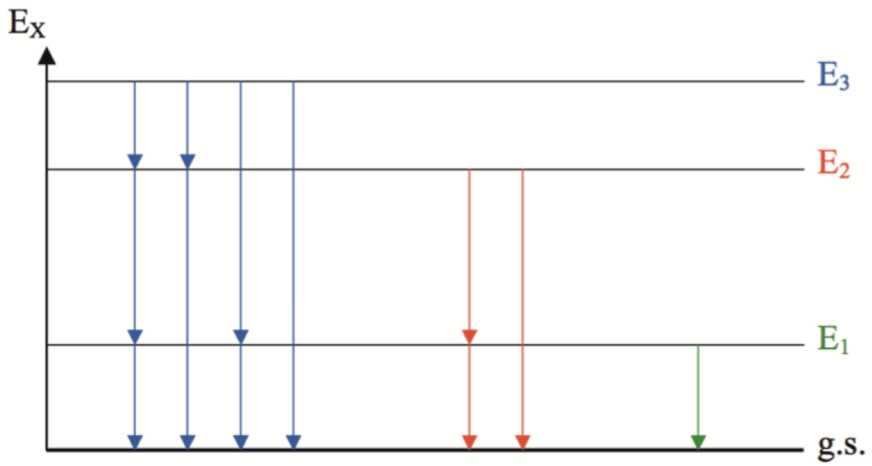

First gen

TALYS is a nuclear reaction program with the objective to provide a complete and accurate simulation of nuclear reactions up to energies of 200 MeV,

Device for Indirect Capture Experiments on Radionuclides (DICER) An instrument for making resonance neutron transmission measurements on very small radioactive samples to tightly constrain their neutron-capture cross sections.

at the Los Alamos Neutron Science Centre (LANSCE)

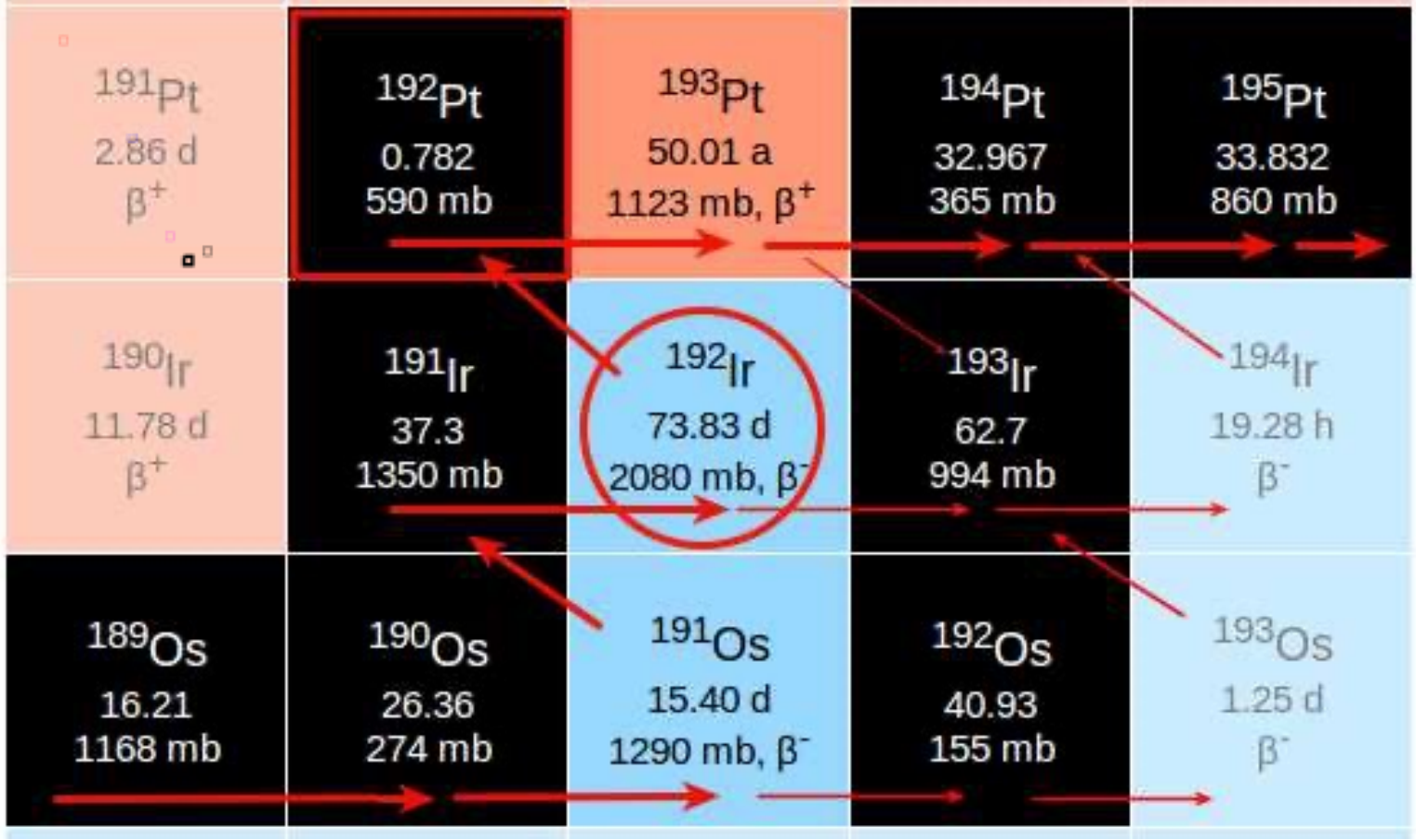

branching points that mainly influence the abundance of s-only isotopes

Abundance distribution

Detector resolution

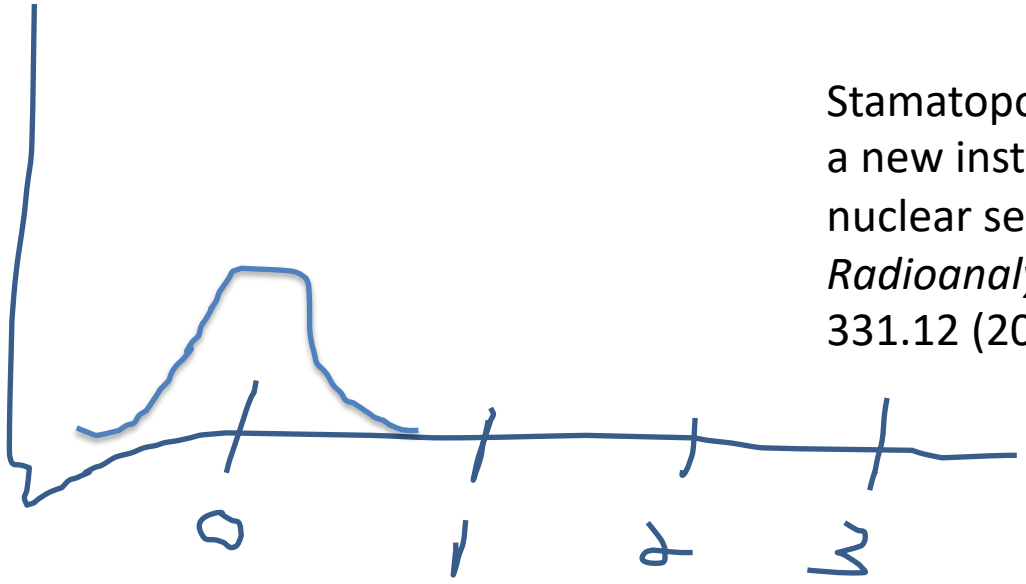

Stamatopoulos, Athanasios, et al. "DICER: a new instrument for nuclear data for nuclear security." *Journal of Radioanalytical and Nuclear Chemistry* 331.12 (2022): 4857-4861.

Check for updates

DICER: a new instrument for nuclear data for nuclear security

Athanasios Stamatopoulos[1] · Artem Matyskin[2] · Paul Koehler[1] · Aaron Couture[1] · Brad DiGiovine[1] · Veronika Mocko[2] · Gencho Rusev[2] · John Ullmann[1] · Christian Vermeulen[2]

Received: 12 April 2022 / Accepted: 2 August 2022 / Published online: 18 August 2022

J^π into any combination of final accessible states μ is given by:

$$T_\gamma^\mu(E, J^\pi) = \sum_{\mu=0,XL} T_{\gamma,XL}^\mu(E, J^\pi) + \int \sum_{XL} T_{\gamma,XL}(E, J^\pi) \times \rho(E - E_\gamma, J^\pi) \cdot dE_\gamma, \qquad (2.22)$$

where the sum $\sum_{\mu=0,XL}$ runs over all experimentally known low-lying discrete states μ with multipolarity XL. The integral runs over the product of the nuclear level density $\rho(E_x - E_\gamma)$ in the continuum and the γ-ray transmission coefficient $T_{\gamma,XL}$, which is directly related to the downward γ-ray strength function $\overrightarrow{f}_{XL}(E_\gamma)$ (see sec. 2.2). The uncertainties associated in any

The absolute normalization parameter B is calculated from $\langle \Gamma_\gamma(S_n, J_T, \pi_T) \rangle$ according to [42]

$$\langle \Gamma_\gamma(S_n, J_T, \pi_T) \rangle = \frac{B}{4\pi D_0} \int_0^{S_n} \mathcal{T}(E_\gamma) \rho(S_n - E_\gamma) dE_\gamma \times \sum_{J=-1}^{1} g\left(S_n - E_\gamma, J_T \pm \frac{1}{2} + J\right), \quad (13)$$

Kheswa 2017 PRC

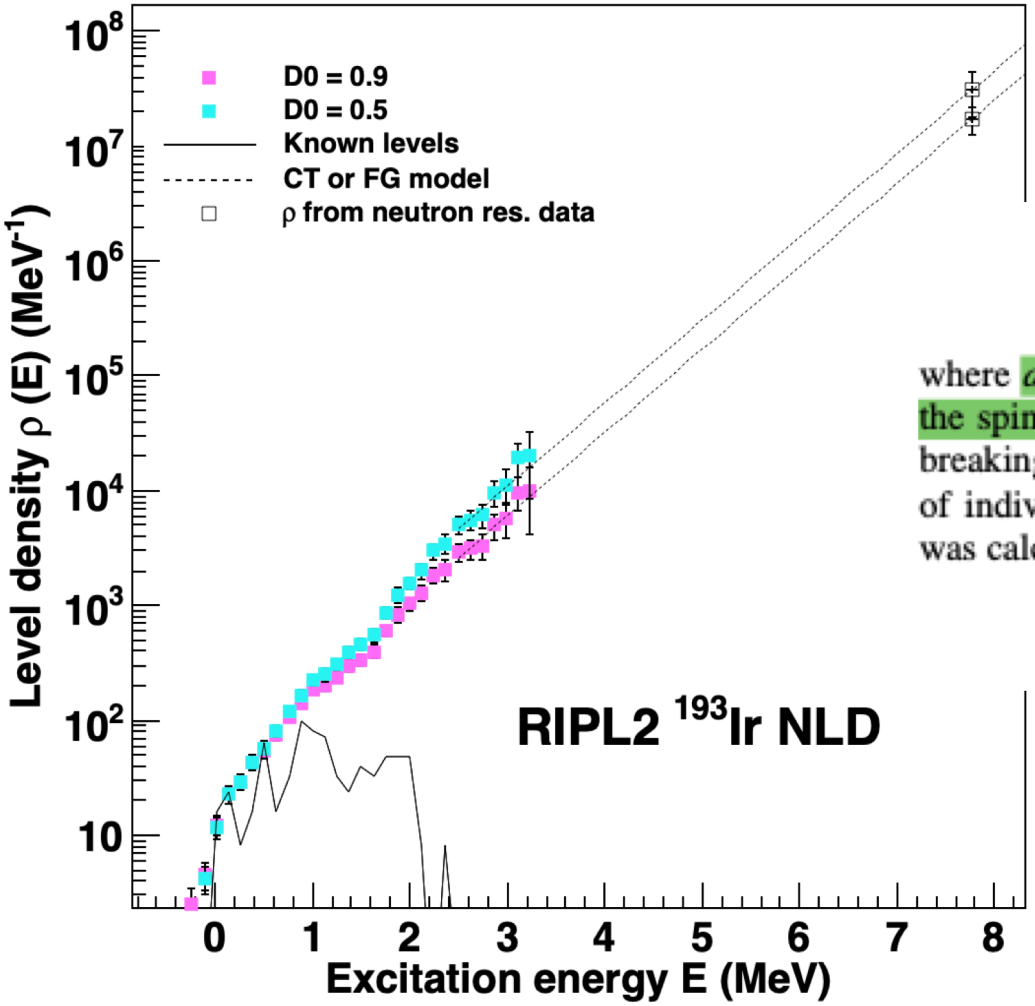

$$\rho(E_x) = \frac{1}{12\sigma\sqrt{2}} \frac{e^{2\sqrt{a(E_x-\delta)}}}{a^{\frac{1}{4}}(E_x-\delta)^{\frac{5}{4}}}, \qquad (10)$$

where a and σ are the level density parameter and width of the spin distribution, respectively. The energy δ accounts for breaking of nucleon pairs that is required before the excitation of individual components. The spin cut-off parameter at S_n was calculated from TALYS with [39]

$$\sigma^2 = 0.01389A^{\frac{5}{3}} \frac{\sqrt{a(E_x-\delta)}}{\bar{a}}, \qquad (11)$$

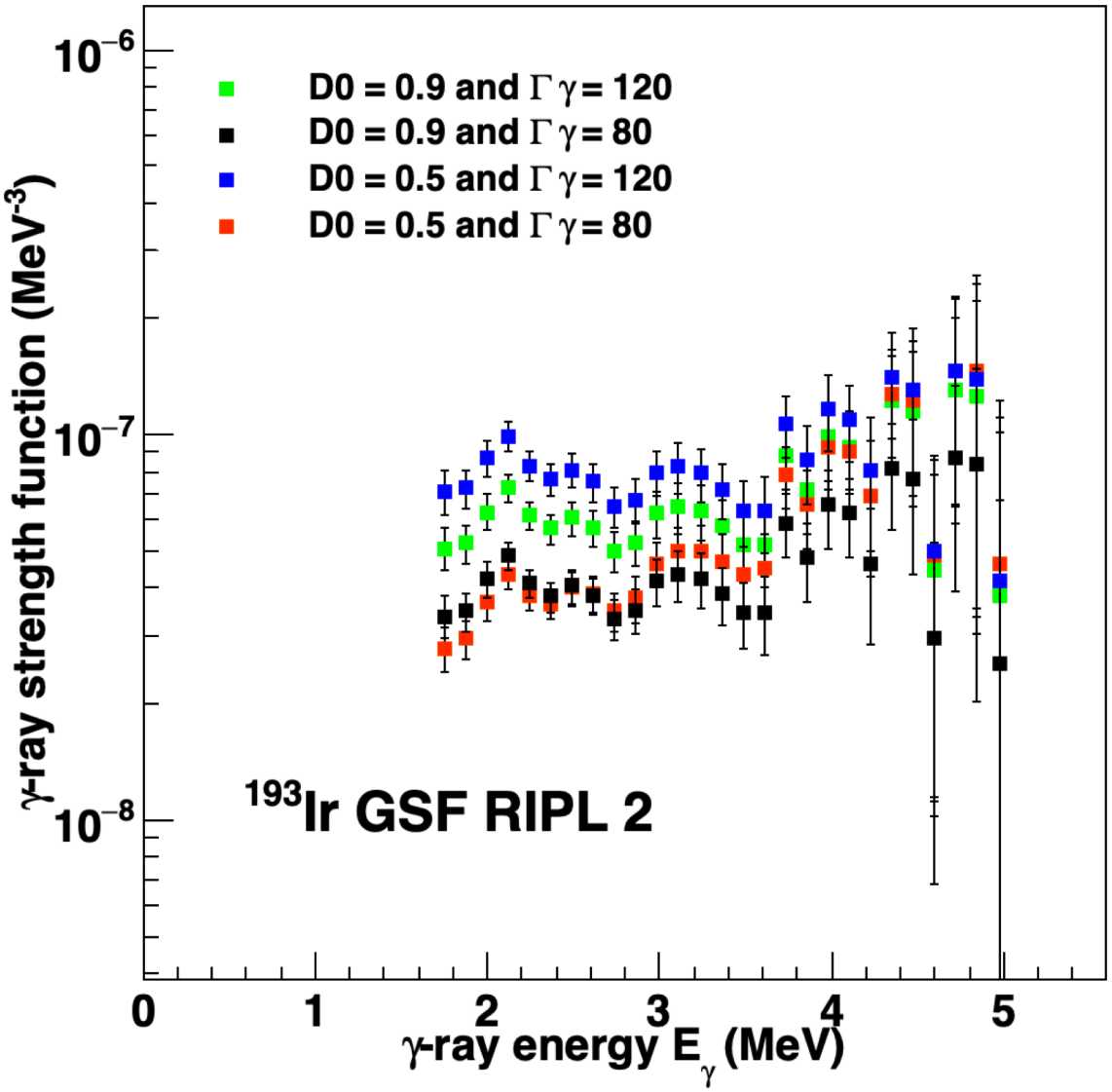

AGB- asymptotic giant Branch stars

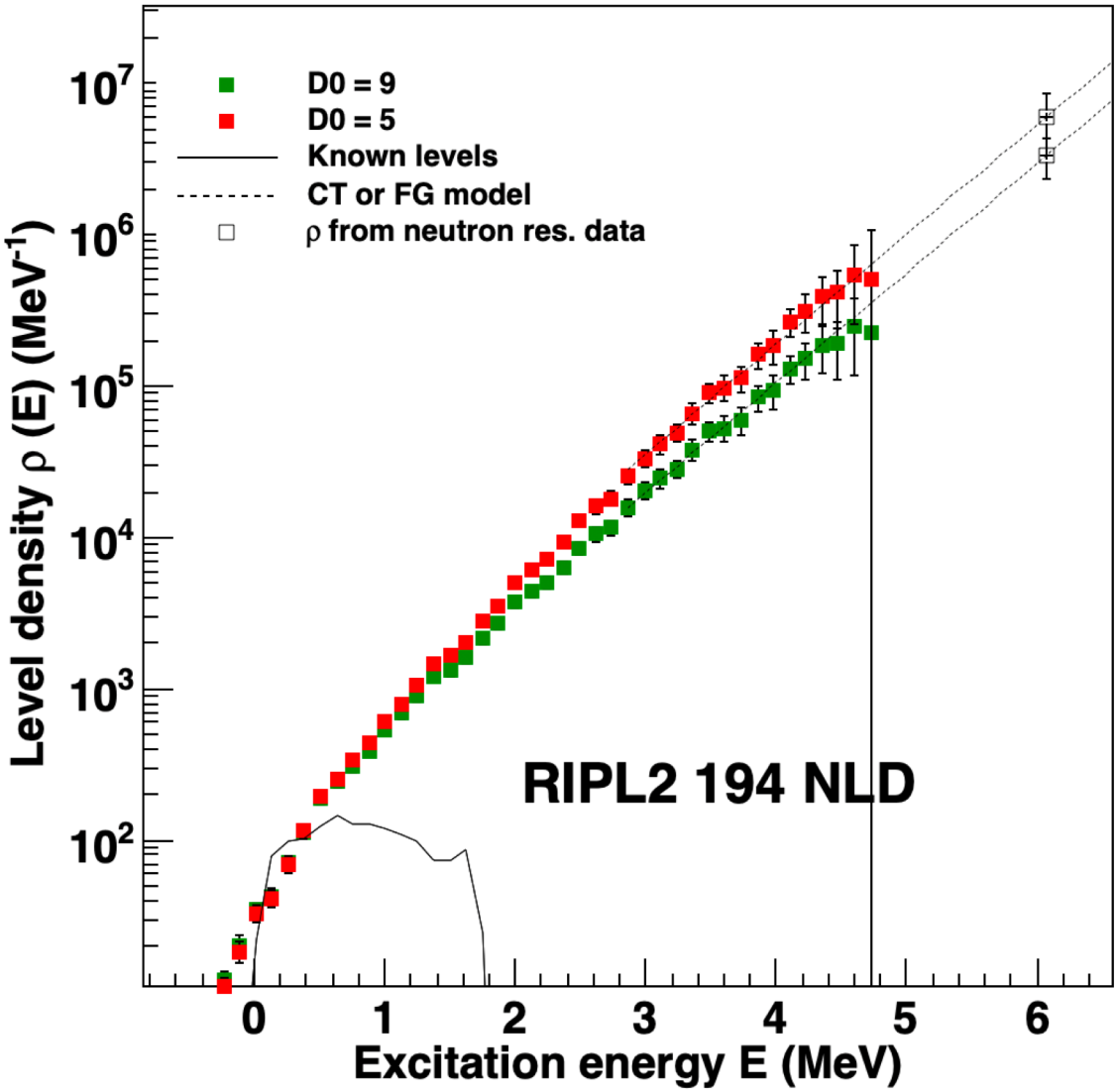
D0 = 9
D0 = 5
Known levels
CT or FG model
ρ from neutron res. data
RIPL2 194 NLD
Level density ρ (E) (MeV-1)
Excitation energy E (MeV)
10^7
10^6
10^5
10^4
10^3
10^2
0
1
2
3
4
5
6

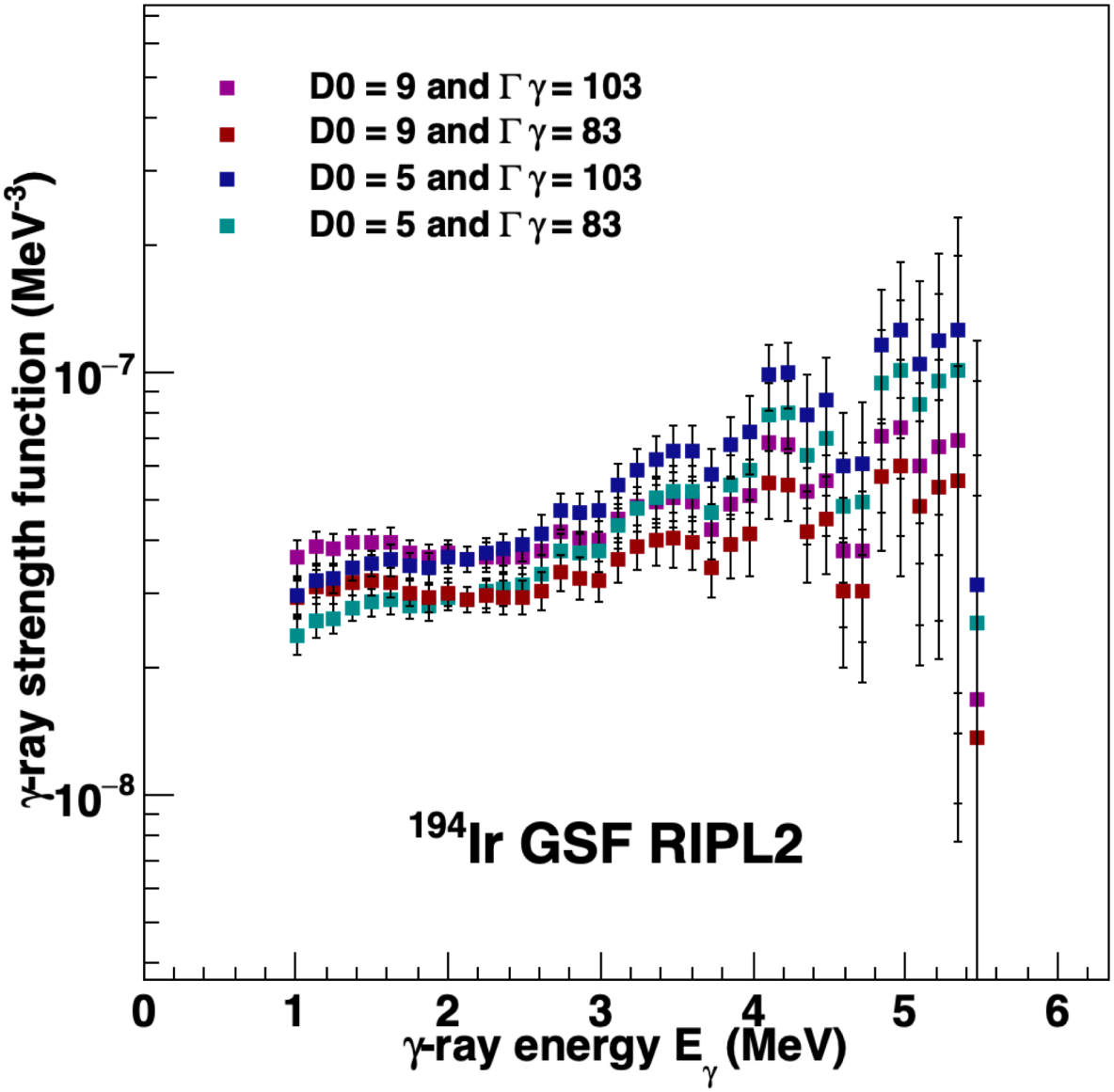
D0 = 9 and Γγ = 103
D0 = 9 and Γγ = 83
D0 = 5 and Γγ = 103
D0 = 5 and Γγ = 83
γ-ray strength function (MeV-3)
10−7
10−8
194Ir GSF RIPL2
0
1
2
3
4
5
6
γ-ray energy Eγ (MeV)

While the radiative neutron capture rate on the stable ^{193}Ir is relatively well constrained by direct measurements of both the cross section and the MACS

The ^{192}Ir(n,γ)^{193}Ir rate used to be affected by a larger uncertainty, typically a factor of 3 within the TALYS upper and lower limits.

The present experimental constraints on the ^{193}Ir NLD and PSF obtained by the Oslo method have allowed us to reduce the corresponding uncertainty to about 20% between the Oslo upper and lower limits.

Such an improvement in the absolute value of the MACS is found to significantly reduce the uncertainty affecting the production of the s-only 192Pt nucleus, as shown in Figure 11. An increase of the ^{192}Ir(n,γ)^{193}Ir obviously decreases the β-branching of 192Ir and consequently decreases the production of 192Pt.

.

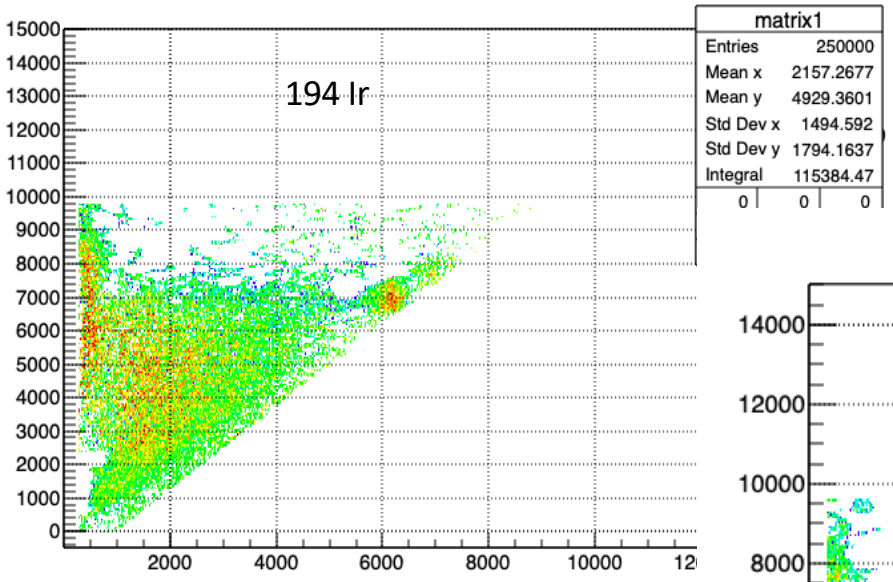
194 Ir
matrix1
Entries 250000
Mean x 2157.2677
Mean y 4929.3601
Std Dev x 1494.592
Std Dev y 1794.1637
Integral 115384.47
0 0 0
15000
14000
13000
12000
11000
10000
9000
8000
7000
6000
5000
4000
3000
2000
1000
0
2000
4000
6000
8000
10000

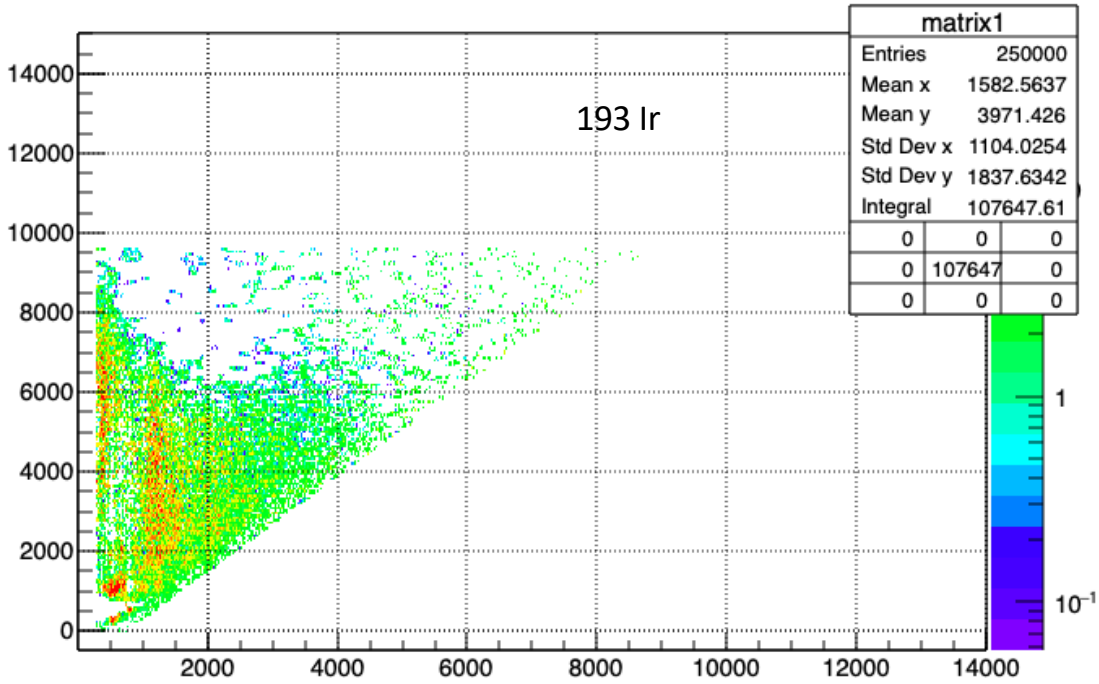
193 Ir
matrix1
Entries 250000
Mean x 1582.5637
Mean y 3971.426
Std Dev x 1104.0254
Std Dev y 1837.6342
Integral 107647.61
0 0 0
0 107647 0
0 0 0
14000
12000
10000
8000
6000
4000
2000
0
2000
4000
6000
8000
10000
12000
14000
1
10^{-1}

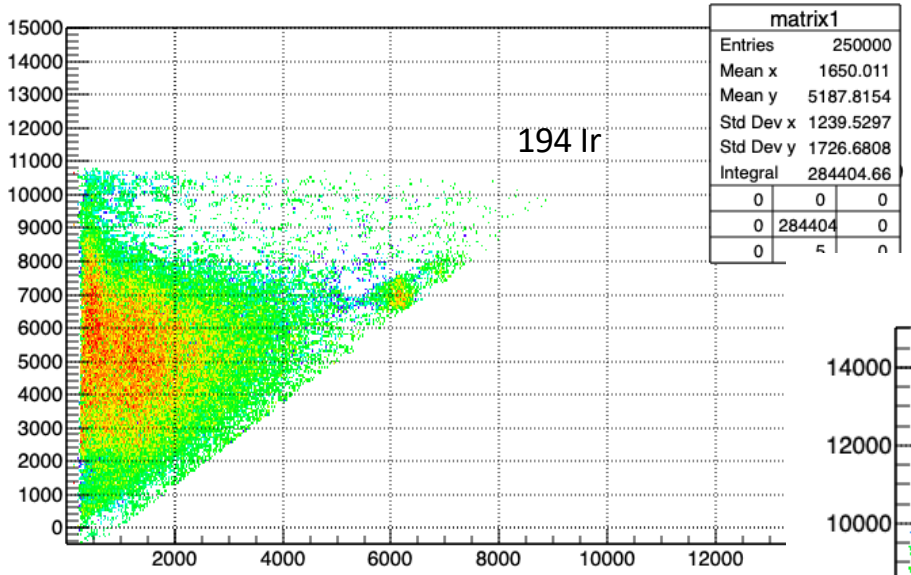
194 Ir
matrix1
Entries 250000
Mean x 1650.011
Mean y 5187.8154
Std Dev x 1239.5297
Std Dev y 1726.6808
Integral 284404.66
0 0 0
0 284404 0
0 5 0
15000
14000
13000
12000
11000
10000
9000
8000
7000
6000
5000
4000
3000
2000
1000
0
2000
4000
6000
8000
10000
12000

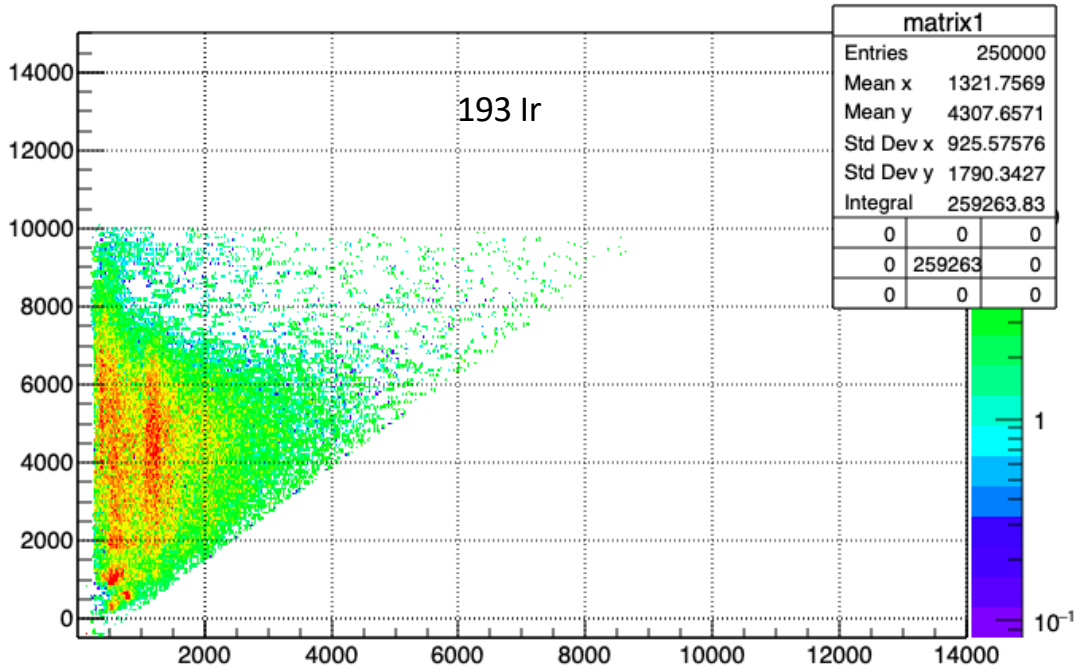
193 Ir
matrix1
Entries 250000
Mean x 1321.7569
Mean y 4307.6571
Std Dev x 925.57576
Std Dev y 1790.3427
Integral 259263.83
0 0 0
0 259263 0
0 0 0
14000
12000
10000
8000
6000
4000
2000
0
2000
4000
6000
8000
10000
12000
14000
1
10^{-1}

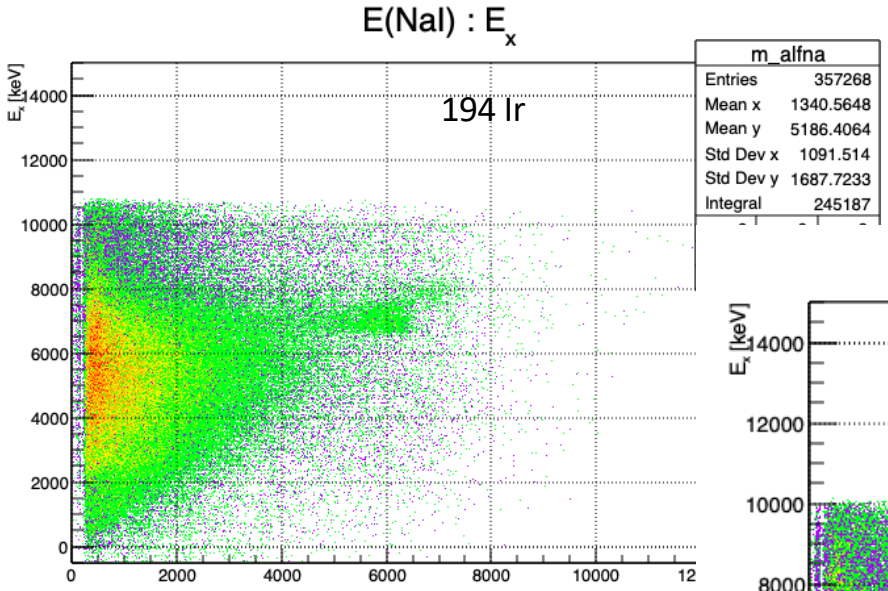
E(NaI) : E_x
194 Ir
m_alfna
Entries 357268
Mean x 1340.5648
Mean y 5186.4064
Std Dev x 1091.514
Std Dev y 1687.7233
Integral 245187
E_x [keV]

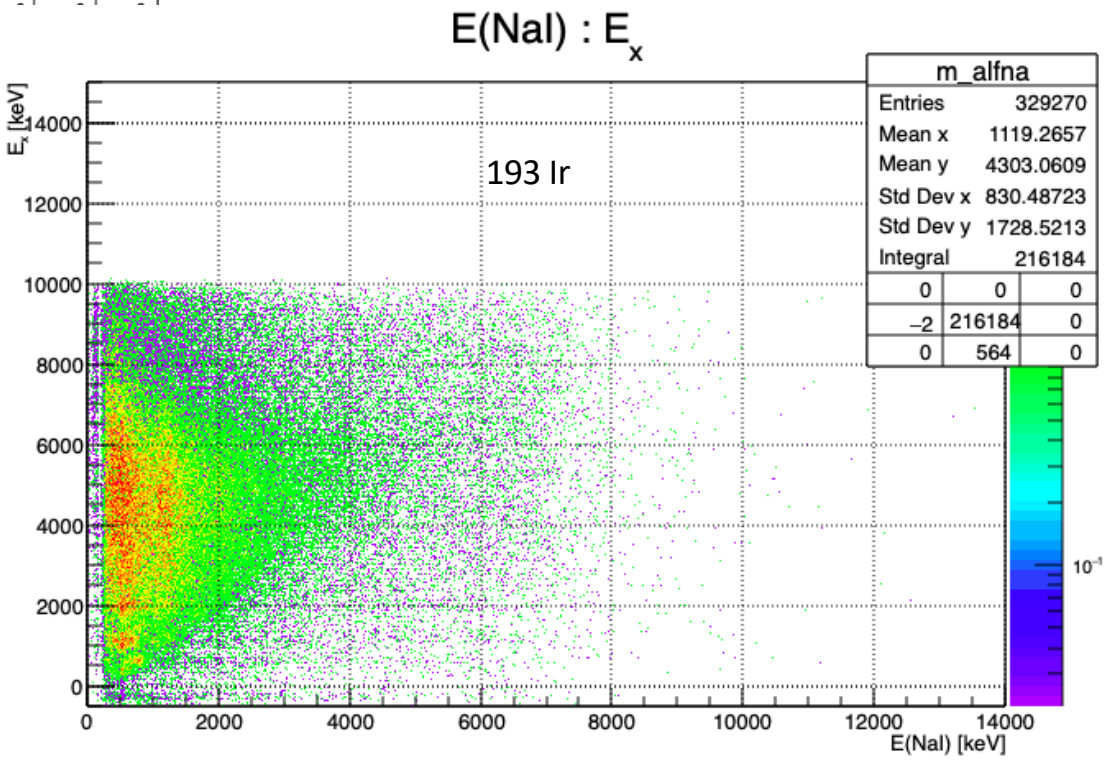
E(NaI) : E_x
193 Ir
m_alfna
Entries 329270
Mean x 1119.2657
Mean y 4303.0609
Std Dev x 830.48723
Std Dev y 1728.5213
Integral 216184
0 0 0
−2 216184 0
0 564 0
E_x [keV]
E(NaI) [keV]

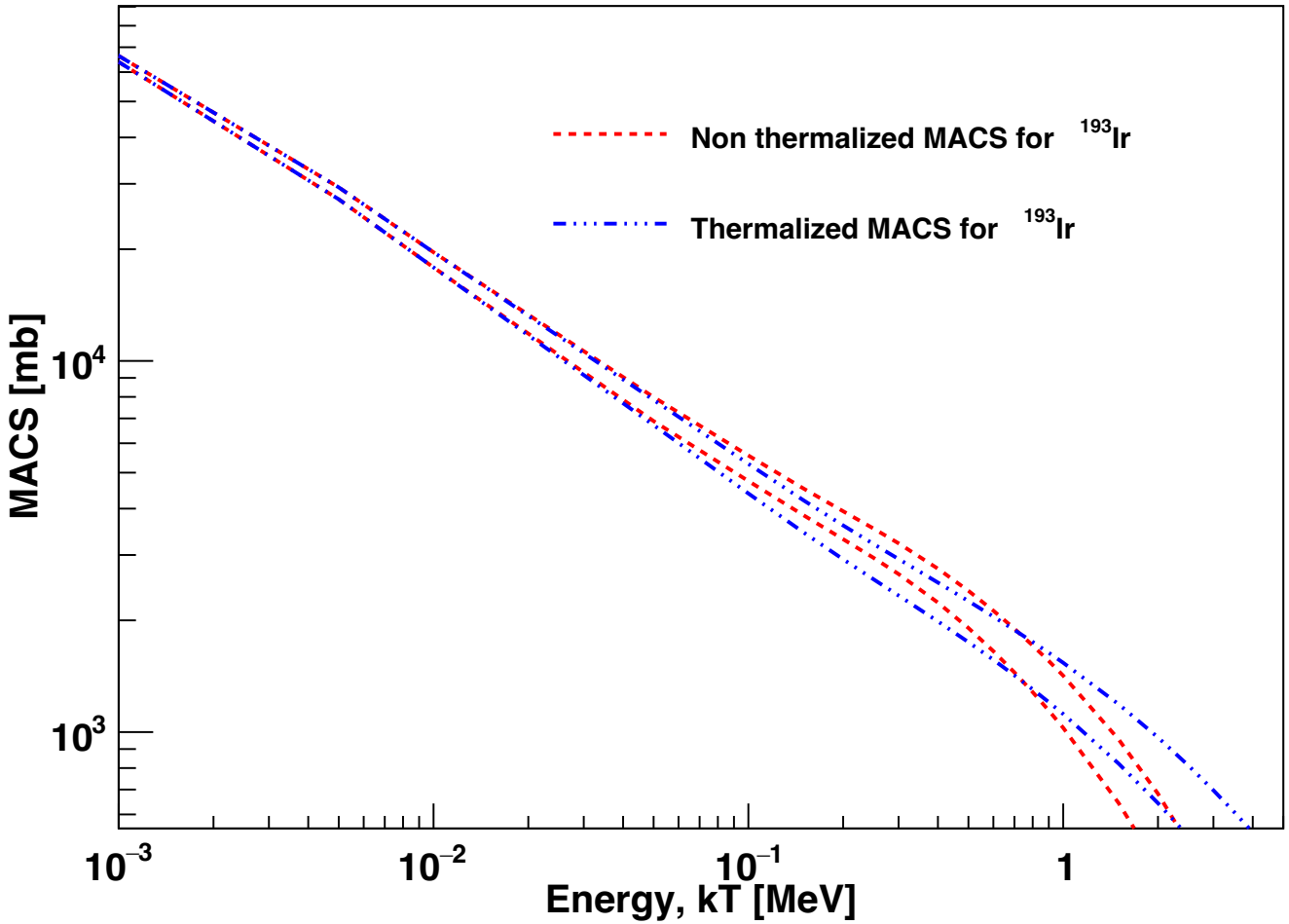

ok the
ck)

ame 1.5
t end at